

# Linear-response density cumulant theory for excited electronic states

Andreas V. Copan\* and Alexander Yu. Sokolov\*

*Department of Chemistry and Biochemistry, The Ohio State University, Columbus, Ohio 43210, United States*

E-mail: avcopan@gmail.com; sokolov.8@osu.edu

## Abstract

We present a linear-response formulation of density cumulant theory (DCT) that provides a balanced and accurate description of many electronic states simultaneously. In the original DCT formulation, only information about a single electronic state (usually, the ground state) is obtained. We discuss the derivation of linear-response DCT, present its implementation for the ODC-12 method (LR-ODC-12), and benchmark its performance for excitation energies in small molecules ( $\text{N}_2$ ,  $\text{CO}$ ,  $\text{HCN}$ ,  $\text{HNC}$ ,  $\text{C}_2\text{H}_2$ , and  $\text{H}_2\text{CO}$ ), as well as challenging excited states in ethylene, butadiene, and hexatriene. For small molecules, LR-ODC-12 shows smaller mean absolute errors in excitation energies than equation-of-motion coupled cluster theory with single and double excitations (EOM-CCSD), relative to the reference data from EOM-CCSDT. In a study of butadiene and hexatriene, LR-ODC-12 correctly describes the relative energies of the singly-excited  $1^1\text{B}_u$  and the doubly-excited  $2^1\text{A}_g$  states, in excellent agreement with highly accurate semistochastic heat-bath configuration interaction results, while EOM-CCSD overestimates the energy of the  $2^1\text{A}_g$  state by almost 1 eV. Our results demonstrate that linear-response DCT is a promising theoretical approach for excited states of molecules.

## 1 Introduction

Accurate simulation of excited electronic states remains one of the major challenges in modern electronic structure theory. *Ab initio* methods for excited states can be divided into single-reference and multi-reference categories, based on their ability to treat static electron correlation. Multi-reference methods<sup>1–18</sup> can correctly describe static correlation in near-degenerate valence orbitals and electronic states with multiple-excitation character, but often lack accurate treatment of important dynamic correlation effects or become computationally very costly when the number of strongly correlated orbitals is large. Meanwhile, single-reference methods<sup>19–33</sup> often provide a compromise between the computational cost and accuracy, and can be used to reliably compute properties of molecules in low-lying electronic states near the equilibrium geometries. In these situations, single-reference equation-of-motion coupled cluster theory (EOM-CC)<sup>21–26</sup> is usually the method of choice, especially when high accuracy is desired.

The EOM-CC methods yield size-intensive excitation energies<sup>28,29</sup> and can be systematically improved by increasing the excitation rank of the cluster operator in the exponential parametrization of the wavefunction. Although EOM-CC is usually formulated in the context of a similarity-transformed Hamiltonian, its excitation energies are equivalent to those obtained from linear-response coupled cluster the-

ory (LR-CC).<sup>27–29</sup> Both EOM-CC and LR-CC are based on non-Hermitian eigenvalue problems, which complicates the computation of molecular properties (e.g., transition dipoles) by requiring evaluation of left and right eigenvectors,<sup>34–37</sup> and may result in an incorrect description of potential energy surfaces in the vicinity of conical intersections where complex excitation energies may be obtained.<sup>38–40</sup> Several Hermitian alternatives to EOM-CC and LR-CC have been proposed to avoid these problems, such as algebraic diagrammatic construction,<sup>41–43</sup> unitary and variational LR-CC,<sup>44–46</sup> similarity-constrained CC,<sup>47</sup> and propagator-based LR-CC.<sup>48,49</sup>

In this work, we present a linear-response formulation of density cumulant theory for excited electronic states. In density cumulant theory (DCT),<sup>50–57</sup> the electronic energy is determined directly in terms of the one-particle reduced density matrix and the density cumulant, i.e. the fully connected part of the two-body reduced density matrix (2-RDM).<sup>58–67</sup> In this regard, DCT is related to approaches based on the variational optimization<sup>62,68–73</sup> or parametrization<sup>74–76</sup> of the 2-RDM. On the other hand, DCT has a close relationship with wavefunction-based electronic structure theories,<sup>53,54</sup> such as linearized, unitary, and variational coupled cluster theory.<sup>77–85</sup> In contrast to variational 2-RDM theory<sup>86–88</sup> and traditional coupled cluster methods,<sup>25,26</sup> DCT naturally combines size-extensivity and a Hermitian energy functional. In addition, the DCT electronic energy is fully optimized with respect to all of its parameters, which greatly simplifies computation of the first-order molecular properties.<sup>89–92</sup> We have successfully applied DCT to a variety of chemical systems with different electronic structure effects (e.g., open-shell, symmetry-breaking, and multi-reference).<sup>54–56,93,94</sup> One limitation of the original DCT formulation is the ability to describe only the lowest-energy state of a particular symmetry (usually, the ground state). By combining DCT with linear response theory, we remove this limitation, providing access to many electronic states simultaneously.

We begin with a brief overview of DCT

(Section 2.1) and linear response theory (Section 2.2). In Section 2.3, we describe the derivation of the linear-response equations for the ODC-12 model (LR-ODC-12). In Section 2.4, we compare the LR-ODC-12 method with linear-response orbital-optimized linearized coupled cluster theory with double excitations (LR-OLCCD), which we derive by linearizing the LR-ODC-12 equations. We outline the computational details in Section 3. In Section 4, we demonstrate that the LR-ODC-12 excitation energies are size-intensive (Section 4.1), test the performance of LR-ODC-12 for the dissociation of H<sub>2</sub> (Section 4.2), benchmark its accuracy for vertical excitation energies of small molecules (Section 4.3), and apply LR-ODC-12 to challenging excited states in ethylene, butadiene, and hexatriene (Section 4.4). We present our conclusions in Section 5.

## 2 Theory

### 2.1 Overview of Density Cumulant Functional Theory

We begin with a brief overview of density cumulant theory (DCT) for a single electronic state. Our starting point is to express the electronic energy as a trace of the one- and anti-symmetrized two-electron integrals ( $h_p^q$  and  $\bar{g}_{pq}^{rs}$ ) with the reduced one- and two-body density matrices ( $\gamma_q^p$  and  $\gamma_{rs}^{pq}$ ):

$$E = h_p^q \gamma_q^p + \frac{1}{4} \bar{g}_{pq}^{rs} \gamma_{rs}^{pq} \quad (1)$$

where summation over the repeated indices is implied. In DCT, the two-body density matrix  $\gamma_{rs}^{pq}$  is expanded in terms of its connected part, the two-body density cumulant ( $\lambda_{rs}^{pq}$ ), and its disconnected part, which is given by an anti-symmetrized product of one-body density matrices:<sup>50</sup>

$$\gamma_{rs}^{pq} = \langle \Psi | a_{rs}^{pq} | \Psi \rangle = \lambda_{rs}^{pq} + P_{(r/s)} \gamma_r^p \gamma_s^q \quad (2)$$

where  $P_{(r/s)} v_{rs} = v_{rs} - v_{sr}$  denotes antisymmetrization and  $a_{rs}^{pq} = a_p^\dagger a_q^\dagger a_s a_r$  is the two-body operator in second quantization. The one-body density matrix  $\gamma_q^p$  is determined from its non-

linear relationship to the cumulant's partial trace:<sup>53</sup>

$$\gamma_q^p = \gamma_r^p \gamma_q^r - \lambda_{qr}^{pr} \quad (3)$$

This allows us to determine the energy (1) from the two-body density cumulant and the spin-orbitals, thereby defining the DCT energy functional. The density cumulant is parametrized by choosing a specific Ansatz for the wavefunction  $|\Psi\rangle$  such that<sup>55</sup>

$$\lambda_{rs}^{pq} = \langle \Psi | a_{rs}^{pq} | \Psi \rangle_c \quad (4)$$

where  $c$  indicates that only fully connected terms are included in the parametrization. Eq. (4) can be considered as a set of  $n$ -representability conditions that ensure that the resulting one- and two-body density matrices represent a physical  $n$ -electron wavefunction. To compute the DCT energy, the functional (1) is made stationary with respect to all of its parameters. Importantly, due to the connected nature of Eq. (4), DCT is both size-consistent and size-extensive for any parametrization of  $|\Psi\rangle$ , and is exact in the limit of a complete parametrization.<sup>55</sup>

In this work, we consider the ODC-12 method,<sup>53,54</sup> which parametrizes the cumulant through a unitary treatment of single excitations and a linear expansion of double excitations:

$$|\Psi\rangle = e^{\hat{T}_1 - \hat{T}_1^\dagger} (1 + \hat{T}_2) |\Phi\rangle \quad (5)$$

$$\hat{T}_1 = \mathbf{t}_1 \cdot \mathbf{a}_1 = t_a^i a_i^a \quad (6)$$

$$\hat{T}_2 = \mathbf{t}_2 \cdot \mathbf{a}_2 = \frac{1}{4} t_{ab}^{ij} a_{ij}^{ab} \quad (7)$$

The exponential singles operator  $e^{\hat{T}_1 - \hat{T}_1^\dagger}$  has the effect of a unitary transformation of the spin-orbital basis and is incorporated in our ODC-12 implementation by optimizing the orbitals.<sup>54</sup> The  $\mathbf{t}_1$  and  $\mathbf{t}_2$  parameters are obtained from the stationarity conditions

$$\frac{\partial E}{\partial \mathbf{t}_1^\dagger} \stackrel{!}{=} 0, \quad \frac{\partial E}{\partial \mathbf{t}_2^\dagger} \stackrel{!}{=} 0 \quad (8)$$

and are used to compute the ODC-12 energy. Explicit equations for the stationarity conditions are given in Refs. 53 and 54. Although in ODC-12 the wavefunction parametrization

is linear with respect to double excitations (Eq. (5)), the ODC-12 energy stationarity conditions are non-linear in  $\mathbf{t}_2$  due to the non-linear relationship between the one-particle density matrix and the density cumulant (Eq. (3)).<sup>53</sup> Neglecting the non-linear  $\mathbf{t}_2$  terms in Eq. (8) results in the equations that define the linearized orbital-optimized coupled cluster doubles method (OLCCD). This method is equivalent to the orbital-optimized coupled electron pair approximation zero (OCEPA<sub>0</sub>).<sup>95</sup>

## 2.2 Linear Response Theory

We now briefly review linear response theory in the quasi-energy formulation.<sup>96</sup> The quasi-energy of a system perturbed by a time-dependent interaction  $\hat{V}f(t)$  is defined as

$$Q(t) = \langle \Psi(t) | \hat{H} + \hat{V}f(t) - i \frac{\partial}{\partial t} | \Psi(t) \rangle \quad (9)$$

where  $\Psi(t)$  is the phase-isolated wavefunction, from which the usual Schrödinger wavefunction can be recovered as  $e^{-i \int_0^t dt' Q(t')} \Psi(t)$ . Assuming that the perturbation is periodic

$$f(t) = \sum_{\omega} f(\omega) e^{-i\omega t} \quad (10)$$

the time average of the quasi-energy over a period of oscillation, denoted as  $\{Q(t)\}$ , is variational with respect to the exact dynamic state.<sup>97</sup> The independent parameters  $\mathbf{u}(t)$  that define such a state can be written using a Fourier expansion

$$\mathbf{u}(t) = \sum_{n=0}^{\infty} \sum_{\omega_1 \dots \omega_n} \mathbf{u}(\omega_1, \dots, \omega_n) e^{-i(\omega_1 + \dots + \omega_n)t} \quad (11)$$

where the outer sum runs over polynomial orders in  $f(t)$ . The stationarity of the time-averaged quasi-energy then implies the following relationship<sup>98</sup>

$$0 = \frac{d}{df(\omega)} \frac{\partial \{Q(t)\}}{\partial \mathbf{u}^\dagger(\omega)} \Big|_{f=0} = \frac{\partial^2 \{Q(t)\}}{\partial \mathbf{u}^\dagger(\omega) \partial \mathbf{u}(\omega)} \frac{\partial \mathbf{u}(\omega)}{\partial f(\omega)} \Big|_{f=0} + \frac{\partial^2 \{Q(t)\}}{\partial \mathbf{u}^\dagger(\omega) \partial f(\omega)} \Big|_{f=0} \quad (12)$$

which constitutes a linear equation for the first-order response of the system to the perturbation. When the frequency  $\omega$  is in resonance with an excitation energy of the system, Eq. (12) will result in an infinite first-order response  $\frac{\partial \mathbf{u}(\omega)}{\partial f(\omega)}$ .

From Eq. (12), we find that these poles occur when the Hessian matrix of the quasi-energy with respect to the wavefunction parameters  $\mathbf{u}(\omega)$  becomes singular. We can express this Hessian matrix in the form:

$$\left. \frac{\partial^2 \{Q(t)\}}{\partial \mathbf{u}^\dagger(\omega) \partial \mathbf{u}(\omega)} \right|_{f=0} \equiv \mathbf{E} - \omega \mathbf{M} \quad (13)$$

where  $\mathbf{E}$  is the Hessian of the time-averaged electronic energy  $\{\langle \Psi(t) | \hat{H} | \Psi(t) \rangle\}$  and  $\omega \mathbf{M}$  is the Hessian of the time-derivative overlap  $\{\langle \Psi(t) | i\dot{\Psi}(t) \rangle\}$ . The excitation energies of the system  $\omega_k$  can therefore be determined by solving the following generalized eigenvalue equation:

$$\mathbf{E} \mathbf{z}_k = \omega_k \mathbf{M} \mathbf{z}_k \quad (14)$$

where  $\mathbf{M}$  serves as the metric matrix. Eq. (14) allows the determination of excitation energies for an arbitrary parametrization of  $|\Psi(t)\rangle$ .

The generalized eigenvectors  $\mathbf{z}_k$  can be used to compute transition properties for excited states. In particular, in the exact linear response theory,<sup>99</sup> the transition strength of the perturbing interaction,  $|\langle \Psi | \hat{V} | \Psi_k \rangle|^2$ , is equal to the complex residue of the following quantity at  $\omega \rightarrow \omega_k$ :

$$\langle \langle \hat{V}; \hat{V} \rangle \rangle_\omega \equiv \mathbf{v}^\dagger \cdot \left. \frac{\partial \mathbf{u}(\omega)}{\partial f(\omega)} \right|_{f=0} \quad (15)$$

This quantity is known as the linear response function and  $\mathbf{v}'$  is termed the property gradient vector,<sup>100</sup> which is defined as follows:

$$\mathbf{v}' \equiv \left. \frac{\partial^2 \{Q(t)\}}{\partial \mathbf{u}^\dagger(\omega) \partial f(\omega)} \right|_{f=0} \quad (16)$$

Substituting Eqs. (13) and (16) into Eq. (12) and decomposing the quasi-energy Hessian as

$$\mathbf{E} - \omega \mathbf{M} = (\mathbf{Z}^\dagger)^{-1} (\mathbf{Z}^\dagger \mathbf{M} \mathbf{Z}) (\mathbf{\Omega} - \omega \mathbf{1}) (\mathbf{Z})^{-1} \quad (17)$$

where  $\mathbf{Z}$  is the matrix of generalized eigenvec-

tors (Eq. (14)) diagonalizing matrices  $\mathbf{E}$  and  $\mathbf{M}$ , and  $\mathbf{\Omega}$  is the diagonal matrix of eigenvalues, we obtain the general formula for the transition strengths:

$$\lim_{\omega \rightarrow \omega_k} (\omega - \omega_k) \langle \langle \hat{V}; \hat{V} \rangle \rangle_\omega = \frac{|\mathbf{z}_k^\dagger \mathbf{v}'|^2}{\mathbf{z}_k^\dagger \mathbf{M} \mathbf{z}_k} \quad (18)$$

In Section 2.3, we will use the quasi-energy formalism to derive equations for the linear-response ODC-12 method (LR-ODC-12).

## 2.3 Linear-Response ODC-12

In the ODC-12 method, the electronic energy Hessian can be written in the following form

$$\mathbf{E} = \begin{pmatrix} \mathbf{A}_{11} & \mathbf{A}_{12} & \mathbf{B}_{11} & \mathbf{B}_{12} \\ \mathbf{A}_{21} & \mathbf{A}_{22} & \mathbf{B}_{21} & \mathbf{B}_{22} \\ \mathbf{B}_{11}^* & \mathbf{B}_{12}^* & \mathbf{A}_{11}^* & \mathbf{A}_{12}^* \\ \mathbf{B}_{21}^* & \mathbf{B}_{22}^* & \mathbf{A}_{21}^* & \mathbf{A}_{22}^* \end{pmatrix} \quad (19)$$

where the submatrices are defined in general as

$$\mathbf{A}_{nm} = \left. \frac{\partial^2 E}{\partial \mathbf{t}_n^\dagger \partial \mathbf{t}_m} \right|_{f=0}, \quad \mathbf{B}_{nm} = \left. \frac{\partial^2 E}{\partial \mathbf{t}_n^\dagger \partial \mathbf{t}_m^*} \right|_{f=0} \quad (20)$$

These complex derivatives relate to the second derivatives of the electronic energy with respect to variations of the orbitals ( $\mathbf{A}_{11}$ ,  $\mathbf{B}_{11}$ ) and cumulant parameters ( $\mathbf{A}_{22}$ ,  $\mathbf{B}_{22}$ ). Similarly, the mixed second derivatives couple variations in the orbitals and cumulant parameters ( $\mathbf{A}_{12}$ ,  $\mathbf{B}_{12}$ ). The metric matrix  $\mathbf{M}$  has a block-diagonal structure, as a consequence of the linear parametrization of the wavefunction in Eq. (5):

$$\mathbf{M} = \begin{pmatrix} \mathbf{S}_{11} & \mathbf{0} & \mathbf{0} & \mathbf{0} \\ \mathbf{0} & \mathbf{1}_2 & \mathbf{0} & \mathbf{0} \\ \mathbf{0} & \mathbf{0} & -\mathbf{S}_{11}^* & \mathbf{0} \\ \mathbf{0} & \mathbf{0} & \mathbf{0} & -\mathbf{1}_2 \end{pmatrix} \quad (21)$$

where  $\mathbf{1}_2 = \langle \Phi | \mathbf{a}_2^\dagger \mathbf{a}_2 | \Phi \rangle$  is an identity matrix over the space of unique two-body excitations and the orbital metric is defined as follows:

$$\omega \mathbf{S}_{11} = \left. \frac{\partial^2 \{\langle \Psi(t) | i\dot{\Psi}(t) \rangle\}}{\partial \mathbf{t}_1^\dagger(\omega) \partial \mathbf{t}_1(\omega)} \right|_{f=0} \quad (22)$$

Equations for all blocks of  $\mathbf{E}$ ,  $\mathbf{M}$ , and the property gradient vector  $\mathbf{v}'$  are shown explicitly in the Supporting Information. The computational cost of solving the LR-ODC-12 equations has  $\mathcal{O}(O^2V^4)$  scaling (where  $O$  and  $V$  are the numbers of occupied and virtual orbitals, respectively), which is the same as the computational scaling of the single-state ODC-12 method. We note that, due to the Hermitian nature of the DCT energy functional (1), the ODC-12 energy Hessian  $\mathbf{E}$  is always symmetric. As a result, in the absence of instabilities (i.e., as long as the Hessian is positive semi-definite), the LR-ODC-12 excitation energies are guaranteed to have real values.

To illustrate the derivation of the LR-ODC-12 energy Hessian, let us consider the diagonal two-body block of  $\mathbf{E}$ . Expressing the energy (1) using the cumulant expansion (2) and differentiating with respect to  $\mathbf{t}_2$ , we obtain:

$$\mathbf{A}_{22} = \frac{\partial^2 E}{\partial \mathbf{t}_2^\dagger \partial \mathbf{t}_2} = f_p^q \frac{\partial^2 \gamma_q^p}{\partial \mathbf{t}_2^\dagger \partial \mathbf{t}_2} + \bar{g}_{pr}^{qs} \frac{\partial \gamma_q^p}{\partial \mathbf{t}_2^\dagger} \frac{\partial \gamma_s^r}{\partial \mathbf{t}_2} + \frac{1}{4} \bar{g}_{pq}^{rs} \frac{\partial^2 \lambda_{rs}^{pq}}{\partial \mathbf{t}_2^\dagger \partial \mathbf{t}_2} \quad (23)$$

where we have introduced the generalized Fock matrix  $f_p^q \equiv h_p^q + \bar{g}_{pr}^{qs} \gamma_s^r$ . The derivatives of the one-body density matrix can be expressed in terms of the derivatives of the density cumulant

$$\mathbf{A}_{22} = \mathcal{F}_p^q \frac{\partial^2 \lambda_{qt}^{pt}}{\partial \mathbf{t}_2^\dagger \partial \mathbf{t}_2} + \mathcal{G}_{pr}^{qs} \frac{\partial \lambda_{qt}^{pt}}{\partial \mathbf{t}_2^\dagger} \frac{\partial \lambda_{su}^{ru}}{\partial \mathbf{t}_2} + \frac{1}{4} \bar{g}_{pq}^{rs} \frac{\partial^2 \lambda_{rs}^{pq}}{\partial \mathbf{t}_2^\dagger \partial \mathbf{t}_2} \quad (24)$$

where the intermediates  $\mathcal{F}_p^q$  and  $\mathcal{G}_{pr}^{qs}$  can be computed using a transformation of the one- and two-electron integrals to the natural spin-orbital basis (see appendix A for details). These cumulant derivatives are straightforward to evaluate from Eqs. (4) and (5) using either algebraic or diagrammatic techniques.

Next, let us outline the derivation of the one-body metric. Substituting Eq. (5) into Eq. (22)

gives

$$\omega \mathbf{S}_{11} = \frac{1}{2} \frac{\partial^2 \{ \langle \Psi | [i\hat{T}_1^\dagger(t), \hat{T}_1(t)] | \Psi \rangle \}}{\partial \mathbf{t}_1^\dagger(\omega) \partial \mathbf{t}_1(\omega)} \Big|_{f=0} - \frac{1}{2} \frac{\partial^2 \{ \langle \Psi | [\hat{T}_1^\dagger(t), i\hat{T}_1(t)] | \Psi \rangle \}}{\partial \mathbf{t}_1^\dagger(\omega) \partial \mathbf{t}_1(\omega)} \Big|_{f=0} \quad (25)$$

where we have assumed that we are working in the variational orbital basis so that  $\hat{T}_1(t)|_{f=0} = 0$ , and  $\Psi = \Psi(t)|_{f=0}$  denotes the ground state wavefunction. Using the Fourier expansion of the  $\mathbf{t}_1(t)$  parameters (Eq. (11)), the gradients of the time derivatives can be evaluated as:

$$\frac{\partial i\hat{T}_1^\dagger(t)}{\partial \mathbf{t}_1^\dagger(\omega)} \Big|_{f=0} = -\omega \mathbf{a}_1^\dagger e^{i\omega t} \quad (26)$$

$$\frac{\partial i\hat{T}_1(t)}{\partial \mathbf{t}_1(\omega)} \Big|_{f=0} = +\omega \mathbf{a}_1 e^{-i\omega t} \quad (27)$$

Substituting Eqs. (26) and (27) into Eq. (25) and evaluating the gradients of  $\hat{T}_1$  and  $\hat{T}_1^\dagger$  similarly gives the final working equation for the one-body metric:

$$\begin{aligned} \omega (\mathbf{S}_{11})_{ia,jb} &= \omega \langle \Psi | [a_a^i, a_j^b] | \Psi \rangle \\ &= \omega (\delta_a^b \gamma_j^i - \delta_j^i \gamma_a^b) \end{aligned} \quad (28)$$

## 2.4 Linear-Response OLCCD

As we discussed in Section 2.1, the orbital-optimized linearized coupled cluster doubles method (OLCCD) can be considered as an approximation to the ODC-12 method where all of the non-linear  $\mathbf{t}_2$  terms are neglected in the stationarity conditions. Similarly, we can formulate the linear-response OLCCD method (LR-OLCCD) by linearizing the LR-ODC-12 equations. This simplifies the expressions for the electronic Hessian blocks that involve the second derivatives with respect to  $\mathbf{t}_2$ . For example, for the  $\mathbf{A}_{22}$  block, we obtain:

$$\mathbf{A}_{22} = (f_0)_i^j \frac{\partial^2 \lambda_{jr}^{ir}}{\partial \mathbf{t}_2^\dagger \partial \mathbf{t}_2} - (f_0)_a^b \frac{\partial^2 \lambda_{br}^{ar}}{\partial \mathbf{t}_2^\dagger \partial \mathbf{t}_2} + \frac{1}{4} \bar{g}_{pq}^{rs} \frac{\partial^2 \lambda_{rs}^{pq}}{\partial \mathbf{t}_2^\dagger \partial \mathbf{t}_2} \quad (29)$$

where  $(f_0)_p^q = h_p^q + \bar{g}_{pi}^{qi}$  is the usual (mean-field) Fock operator. Comparing Eq. (29) with Eq. (24) from the LR-ODC-12 method, we observe that the former equation can be obtained from the latter by replacing the  $\mathcal{F}_p^q$  intermediates with the mean-field Fock matrix elements and ignoring the term that depends on  $\mathcal{G}_{pr}^{qs}$ . These simplifications arise from the fact that the  $\mathcal{F}_p^q$  and  $\mathcal{G}_{pr}^{qs}$  intermediates contain high-order  $\mathbf{t}_2$  contributions that are not included in the linearized LR-OLCCD formulation (see appendix A and Ref. 53 for details). For the  $\mathbf{B}_{22}$  block, we find that all of the Hessian elements are zero. A complete set of working equations for LR-OLCCD is given in the Supporting Information.

### 3 Computational Details

The LR-ODC-12 and LR-OLCCD methods were implemented as a standalone Python program, which was interfaced with PSI4<sup>101</sup> and PYSCF<sup>102</sup> to obtain the one- and two-electron integrals. To compute excitation energies, our implementation utilizes the multi-root Davidson algorithm,<sup>103,104</sup> which solves the generalized eigenvalue problem (14) by progressively growing an expansion space for the  $n_{\text{root}}$  lowest generalized eigenvectors of the electronic Hessian and the metric matrix. A key feature of this algorithm is that it avoids storing the Hessian and metric matrices, significantly reducing the amount of memory required by the computations. Our implementation of the energy Hessian was validated by computing the static response function for a dipole perturbation (i.e., the dipole polarizability):

$$\langle\langle \hat{V}; \hat{V} \rangle\rangle_0 = -\mathbf{v}'^t \mathbf{E}^{-1} \mathbf{v}' \quad (30)$$

This quantity can be evaluated numerically as a derivative of the ground state energy

$$\langle\langle \hat{V}; \hat{V} \rangle\rangle_0 = \left. \frac{d^2 E}{df^2} \right|_{f=0} \quad (31)$$

by perturbing the one-electron integrals  $h_p^q \leftarrow h_p^q + f v_p^q$  with the integrals of the perturbing dipole operator ( $v_p^q$ ), and solving the ODC-12

(or OLCCD) equations for different values of  $f$ . For the dipole polarizability of the water molecule along its  $C_2$  symmetry axis, the values of  $\langle\langle \hat{V}; \hat{V} \rangle\rangle_0$  computed using Eqs. (30) and (31) matched to  $10^{-9}$  a.u.

We used Q-CHEM 4.4<sup>105</sup> to obtain results from equation-of-motion coupled cluster theory with single and double excitations (EOM-CCSD) and EOM-CCSD with triple excitations in the EOM part [EOM-CC(2,3)]. The MRCC program<sup>106</sup> was used to obtain results for equation-of-motion coupled cluster theory with up to full triple excitations (EOM-CCSDT). All electrons were correlated in all computations. We used tight convergence parameters in all ground-state ( $10^{-8} E_h$ ) and excited-state computations ( $10^{-5} E_h$ ). In Sections 4.2 and 4.3, the augmented aug-cc-pVTZ and d-aug-cc-pVTZ basis sets of Dunning and co-workers were employed.<sup>107</sup> For alkenes (Section 4.4), the ANO-L-pVXZ ( $X = D, T$ ) basis sets<sup>108</sup> were used as in Ref. 109. To compute vertical excitation energies in Section 4.3, geometries of molecules were optimized using ODC-12 (for LR-ODC-12), OLCCD (for LR-OLCCD), or CCSD [for EOM-CCSD, EOM-CC(2,3), and EOM-CCSDT]. For the alkenes in Section 4.4, frozen-core MP2/cc-pVQZ geometries were used as in Refs. 109 and 110.

## 4 Results

### 4.1 Size-Intensivity of the LR-ODC-12 Energies

In Section 2.1, we mentioned that all DCT methods are by construction *size-extensive*, meaning that their electronic energies scale linearly with the number of electrons. In this section, we demonstrate that the LR-ODC-12 excitation energies are *size-intensive*, i.e. they satisfy the following property:  $E(A^* + B) = E(A^*) + E(B)$ , where  $A$  and  $B$  are two noninteracting fragments in their corresponding ground states and  $A^*$  is the fragment  $A$  in an excited state. Table 1 shows the ODC-12 ground-state energies and the LR-ODC-12 excitation energies for the CO molecule and noninteracting

Table 1: Ground-state energies (in  $E_h$ ) and vertical excitation energies (in eV) for the four lowest-energy excited states of the CO molecule and noninteracting systems of CO with Ne atoms ( $\text{CO} + n\text{Ne}$ ,  $n = 1, 2, 3$ ) computed using the ODC-12 and LR-ODC-12 methods (cc-pVDZ basis set). The noninteracting systems were separated from each other by 10000 Å and the C–O bond distance was set to 1.12547 Å. Results demonstrate size-intensivity of the LR-ODC-12 excitation energies.

	CO	CO + Ne	CO + 2Ne	CO + 3Ne
$X^1\Sigma_g^+$	-113.051282	-241.730913	-370.410543	-499.090174
$^3\Pi$	6.48596	6.48596	6.48596	6.48596
$^3\Sigma^+$	8.41225	8.41225	8.41225	8.41225
$^1\Pi$	8.90866	8.90866	8.90866	8.90866
$^3\Delta$	9.33189	9.33189	9.33189	9.33189

systems composed of CO and the neon atoms separated by 10000 Å ( $\text{CO} + n\text{Ne}$ ,  $n = 1, 2, 3$ ). The scaling of the ODC-12 energies with the number of electrons for the ground  $X^1\Sigma_g^+$  electronic state is perfectly linear up to  $10^{-8} E_h$ , which is the convergence parameter used in our ODC-12 computations. Upon the addition of the neon atoms, the excitation energies of the CO molecule remain constant up to the convergence threshold set in LR-ODC-12 ( $10^{-6}$  eV). These results provide numerical evidence that the LR-ODC-12 excitation energies are size-intensive.

## 4.2 H<sub>2</sub> Dissociation

One of the desirable properties of an electronic structure method is exactness for two-electron systems. While the ODC-12 method is not exact for two-electron systems, it has been shown to provide a very good description of the ground-state H<sub>2</sub> dissociation curve, with errors of  $\sim 1$  kcal mol<sup>-1</sup> with respect to full configuration interaction (FCI) near the dissociation limit.<sup>54</sup> Here, we investigate the performance of LR-ODC-12 for the excited states of H<sub>2</sub>. Figure 1a shows the errors in vertical excitation energies for six lowest-lying electronic states as a function of the H–H distance, relative to FCI. The FCI energies were computed using the EOM-CCSD method, which is exact for two-electron systems. At the equilibrium geometry ( $r_e = 0.742$  Å) the errors in excitation energies for all states do not exceed 0.02 eV. Be-

tween 0.6 and 1.45 Å ( $r \approx 2r_e$ ), the LR-ODC-12 excitation energies remain in good agreement with FCI, with errors less than 0.1 eV for all states. In this range, the largest error is observed for the  $^3\Sigma_u^+$  state. For  $r \geq 1.5$  Å, the error in the  $^1\Sigma_g^+$  excited state energy rapidly increases from 0.10 eV (at 1.5 Å) to 2.13 eV (at 2.35 Å), while for other states the errors increase much more slowly. Analysis of the FCI wavefunction for the  $^1\Sigma_g^+$  state shows a significant contribution from the  $(1\sigma_g)^2 \rightarrow (1\sigma_u)^2$  double excitation already at  $r = 1.55$  Å. This contribution becomes dominant for  $r \geq 1.75$  Å. Thus, the large LR-ODC-12 errors observed for the  $^1\Sigma_g^+$  state are likely due to the increasingly large double-excitation character of this electronic state at long H–H bond distances. The second largest error near the dissociation is observed for the  $^3\Sigma_u^+$  state (0.43 eV). For other electronic states, smaller errors of  $\sim 0.25$  eV are observed near the dissociation.

The importance of the non-linear terms in the LR-ODC-12 equations can be investigated by comparing the LR-ODC-12 and LR-OLCCD results. Figure 1b shows the errors in the LR-OLCCD vertical excitation energies as a function of the H–H bond length. Although near the equilibrium geometry the performance of LR-OLCCD and LR-ODC-12 is similar, the LR-OLCCD errors increase much faster with increasing H–H distance compared to LR-ODC-12. At  $r = 1.3$  Å, the LR-OLCCD error for the  $^3\Sigma_u^+$  state (0.4 eV) is almost six times larger than the corresponding error from LR-ODC-12

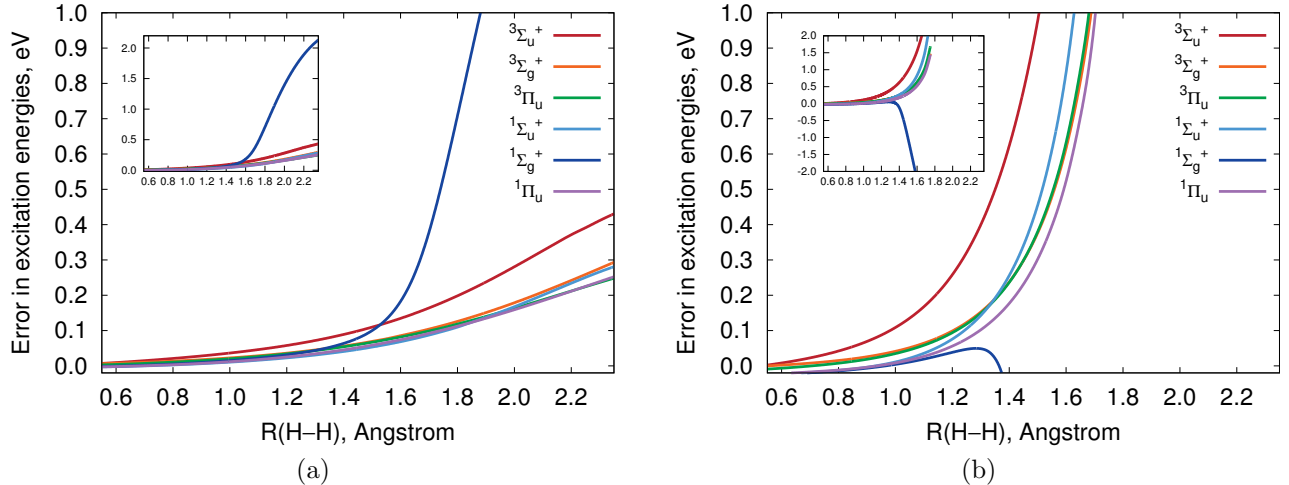


Figure 1: Errors in vertical excitation energies (eV) for six lowest-lying electronic states of  $\text{H}_2$  computed using LR-ODC-12 (1a) and LR-OLCCD (1b) as a function of the H–H bond length, relative to full configuration interaction. All methods employed the d-aug-cc-pvtz basis set. In each figure, the inset shows the same plot for a larger range of errors.

(0.07 eV). For  $r \geq 1.35$  Å, the LR-OLCCD errors for all excitation energies show very steep increase in magnitude, ranging from 1.5 to 4.7 eV already at  $r = 1.75$  Å. We were unable to converge the LR-OLCCD equations for  $r \geq 1.80$  Å. Overall, our results demonstrate that the non-linear terms in LR-ODC-12 significantly improve the description of the excited states at long H–H distances where the electron correlation effects are stronger.

### 4.3 Benchmark: Small Molecules

Here, we benchmark the performance of LR-ODC-12 for vertical excitation energies in several small molecules:  $\text{N}_2$ ,  $\text{CO}$ ,  $\text{HCN}$ ,  $\text{HNC}$ ,  $\text{C}_2\text{H}_2$ , and  $\text{H}_2\text{CO}$ . Tables 2 and 3 show the errors in excitation energies computed using EOM-CCSD, LR-OLCCD, and LR-ODC-12 for the singlet and triplet excited states, respectively, relative to the results from EOM-CCSDT. To measure the performance of each method, we computed the mean absolute errors ( $\Delta_{\text{MAE}}$ ) and the standard deviations from the average signed error ( $\Delta_{\text{STD}}$ ), shown in Figure 2.

For the singlet electronic states (Table 2), the excitation energies computed using LR-ODC-12 are in better agreement with EOM-CCSDT than those obtained from EOM-CCSD, on average. This is evidenced by  $\Delta_{\text{MAE}}$ , which is

Figure 2: Mean absolute deviations ( $\Delta_{\text{MAE}}$ ) and standard deviations from the mean signed error ( $\Delta_{\text{STD}}$ ) for vertical excitation energies (Tables 2 and 3) computed using LR-OLCCD, LR-ODC-12, and EOM-CCSD, relative to EOM-CCSDT (aug-cc-pVTZ basis set). The  $\Delta_{\text{MAE}}$  value is represented as a height of each colored box, while the  $\Delta_{\text{STD}}$  value is depicted as a radius of the black vertical bar.

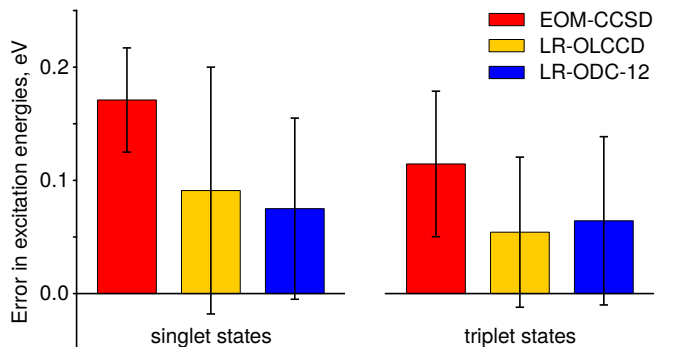




Table 2: Errors in vertical excitation energies (eV) for singlet states computed using LR-OLCCD, LR-ODC-12, and EOM-CCSD, relative to EOM-CCSDT (aug-cc-pVTZ basis set). All electrons were correlated in all computations. Also shown are mean absolute errors ( $\Delta_{\text{MAE}}$ ) and standard deviations ( $\Delta_{\text{STD}}$ ) computed for each method.

		$\Delta\text{EOM-CCSD}$	$\Delta\text{LR-OLCCD}$	$\Delta\text{LR-ODC-12}$	$\text{EOM-CCSDT}$
$\text{N}_2$	$^1\Pi_g$	0.18	0.08	0.20	9.29
	$^1\Sigma_u^-$	0.23	0.15	0.09	9.84
	$^1\Delta_u$	0.26	0.14	0.10	10.26
$\text{CO}$	$^1\Pi$	0.16	0.09	0.17	8.46
	$^1\Sigma^-$	0.19	-0.10	-0.01	9.89
	$^1\Delta$	0.19	-0.22	-0.05	10.03
$\text{HCN}$	$^1\Sigma^-$	0.16	0.05	0.00	8.25
	$^1\Delta$	0.17	0.04	0.01	8.61
	$^1\Pi$	0.17	0.05	0.20	9.12
$\text{HNC}$	$^1\Pi$	0.15	-0.01	0.10	8.13
	$^1\Sigma^+$	0.24	0.05	0.12	8.46
	$^1\Sigma^-$	0.15	-0.09	0.04	8.67
	$^1\Delta$	0.15	-0.18	-0.03	8.84
$\text{C}_2\text{H}_2$	$^1\Sigma_u^-$	0.12	0.06	0.02	7.11
	$^1\Delta_u$	0.10	0.07	0.03	7.45
$\text{H}_2\text{CO}$	$^1\text{A}_2$	0.10	-0.07	0.02	3.95
$\Delta_{\text{MAE}}$		0.17	0.09	0.08	
$\Delta_{\text{STD}}$		0.05	0.11	0.08	

smaller for LR-ODC-12 compared to EOM-CCSD by a factor of two ( $\Delta_{\text{MAE}} = 0.08$  and  $0.17$  eV, respectively). The LR-ODC-12 errors exceed  $0.10$  eV for only four states, with a maximum error of  $0.20$  eV. EOM-CCSD has a minimum error of  $0.10$  eV, shows errors greater than  $0.10$  eV for 14 states, and has a maximum error of  $0.26$  eV. EOM-CCSD shows a somewhat smaller  $\Delta_{\text{STD}}$  compared to that of LR-ODC-12 ( $\Delta_{\text{STD}} = 0.05$  and  $0.08$  eV, respectively).

For the triplet states (Table 3), LR-ODC-12 is again superior to EOM-CCSD, on average, with  $\Delta_{\text{MAE}} = 0.06$  and  $0.11$  eV for the two methods, respectively. LR-ODC-12 has errors larger than  $0.10$  eV for five states with a maximum error of  $0.14$  eV, whereas EOM-CCSD exceeds  $0.10$  eV error for 12 states and shows a maximum error of  $0.28$  eV. For linear molecules, EOM-CCSD exhibits consistently poor results for the  $^3\Sigma^-$  electronic states, while the performance of LR-ODC-12 for different electronic states is similar. Notably, all EOM-CCSD excitation energies overestimate the EOM-CCSDT

values, while the LR-ODC-12 energies are centered around the reference energies, suggesting that LR-ODC-12 provides a more balanced description of the ground and excited states.

Comparing LR-ODC-12 with LR-OLCCD, we see that both methods show very similar results for the triplet states ( $\Delta_{\text{MAE}} = 0.06$  and  $0.05$  eV, respectively), with noticeable differences observed only for the  $^3\Sigma^-$  states. For the singlet electronic states, LR-OLCCD shows a somewhat larger  $\Delta_{\text{MAE}} = 0.09$  eV and  $\Delta_{\text{STD}} = 0.11$  eV compared to LR-ODC-12 ( $\Delta_{\text{MAE}} = 0.08$  eV and  $\Delta_{\text{STD}} = 0.08$  eV). In this case, significant differences are observed for the  $^1\Pi$  states of  $\text{N}_2$  and  $\text{HCN}$ ,  $^1\Sigma^-$  of  $\text{HNC}$ , and  $^1\Delta$  of  $\text{CO}$  and  $\text{HNC}$ , indicating that the non-linear terms included in LR-ODC-12 are important for these electronic states.

Table 3: Errors in vertical excitation energies (eV) for triplet states computed using LR-OLCCD, LR-ODC-12, and EOM-CCSD, relative to EOM-CCSDT (aug-cc-pVTZ basis set). All electrons were correlated in all computations. Also shown are mean absolute errors ( $\Delta_{\text{MAE}}$ ) and standard deviations ( $\Delta_{\text{STD}}$ ) computed for each method.

		$\Delta\text{EOM-CCSD}$	$\Delta\text{LR-OLCCD}$	$\Delta\text{LR-ODC-12}$	$\text{EOM-CCSDT}$
$\text{N}_2$	$^3\Sigma_u^+$	0.11	0.04	-0.02	7.63
	$^3\Pi_g$	0.15	0.06	0.11	8.00
	$^3\Delta_u$	0.17	0.08	0.03	8.82
	$^3\Sigma_u^-$	0.28	0.03	0.01	9.63
	$^3\Pi_u$	0.14	-0.01	0.10	11.18
$\text{CO}$	$^3\Pi$	0.12	0.06	0.08	6.27
	$^3\Sigma^+$	0.05	-0.03	-0.03	8.38
	$^3\Delta$	0.11	-0.07	-0.03	9.21
	$^3\Sigma^-$	0.19	-0.18	-0.06	9.72 <sup>a</sup>
$\text{HCN}$	$^3\Sigma^+$	0.05	-0.04	-0.10	6.40
	$^3\Delta$	0.13	-0.02	-0.06	7.40
	$^3\Pi$	0.10	0.08	0.06	8.01
	$^3\Sigma^-$	0.16	-0.10	-0.05	8.15 <sup>a</sup>
$\text{HNC}$	$^3\Pi$	0.09	0.00	0.03	6.06
	$^3\Sigma^+$	0.04	-0.09	-0.11	7.20
	$^3\Delta$	0.10	-0.14	-0.11	8.02
	$^3\Sigma^+$	0.22	-0.05	0.04	8.38
	$^3\Sigma^-$	0.15	-0.02	0.11	8.56 <sup>a</sup>
$\text{C}_2\text{H}_2$	$^3\Sigma_u^+$	0.01	-0.02	-0.08	5.52
	$^3\Delta_u$	0.08	-0.02	-0.05	6.41
	$^3\Sigma_u^-$	0.10	-0.03	-0.05	7.10 <sup>a</sup>
$\text{H}_2\text{CO}$	$^3\text{A}_2$	0.04	-0.02	0.01	3.56
	$^3\text{A}_1$	0.02	-0.06	-0.14	6.06
$\Delta_{\text{MAE}}$		0.11	0.05	0.06	
$\Delta_{\text{STD}}$		0.06	0.07	0.07	

<sup>a</sup> For CO, HCN, HNC, and  $\text{C}_2\text{H}_2$ , the  $^3\Sigma^-$  ( $^3\Sigma_u^-$ ) excitation energies were obtained from EOM-CC(2,3), which energies were shifted to reproduce the EOM-CCSDT energy for the  $^1\Sigma^-$  ( $^1\Sigma_u^-$ ) state.

#### 4.4 Ethylene, Butadiene, and Hexatriene

Finally, we apply the LR-ODC-12 method to challenging excited states of ethylene ( $\text{C}_2\text{H}_4$ ), butadiene ( $\text{C}_4\text{H}_6$ ), and hexatriene ( $\text{C}_6\text{H}_8$ ). A reliable description of these electronic states requires an accurate treatment of electron correlation.<sup>109,110,112–126</sup> All three molecules feature a dipole-allowed  $1^1\text{B}_u$  (or  $1^1\text{B}_{1u}$ ) state that is well described as a  $\pi - \pi^*$  excitation, but requires a very accurate description of dynamic correlation between the  $\sigma$  and  $\pi$  electrons. In buta-

diene and hexatriene, the  $1^1\text{B}_u$  state is near-degenerate with a dipole-forbidden  $2^1\text{A}_g$  state that has a substantial double-excitation character, requiring the description of static correlation in the  $\pi$  and  $\pi^*$  orbitals.<sup>120–122</sup> For this reason, the relative energies and ordering of the  $1^1\text{B}_u$  and  $2^1\text{A}_g$  states are very sensitive to various levels of theory. For example, single-reference methods truncated to single and double excitations describe the  $1^1\text{B}_u$  state more accurately than the  $2^1\text{A}_g$  state, while multi-reference methods are more reliable for the  $2^1\text{A}_g$  state, missing important dynamic correlation

Table 4: Vertical excitation energies computed using LR-OLCCD, LR-ODC-12, and EOM-CCSD for the low-lying electronic states of ethylene ( $\text{C}_2\text{H}_4$ ), butadiene ( $\text{C}_4\text{H}_6$ ), and hexatriene ( $\text{C}_6\text{H}_8$ ). Computations employed the ANO-L-pVDZ (for  $\text{C}_4\text{H}_6$  and  $\text{C}_6\text{H}_8$ ) and ANO-L-pVTZ (for  $\text{C}_2\text{H}_4$ ) basis sets and the MP2/cc-pVQZ optimized geometries. For LR-OLCCD and LR-ODC-12, oscillator strengths of the allowed transitions are given in parentheses. All electrons were correlated in all computations.

		EOM-CCSD	LR-OLCCD	LR-ODC-12	SHCI <sup>a</sup>
$\text{C}_2\text{H}_4$	$1^3\text{B}_{1u}$	4.46	4.66	4.52	4.59
	$1^1\text{B}_{1u}$	8.14	8.20 (1.8)	8.13 (1.9)	8.05
$\text{C}_4\text{H}_6$	$1^3\text{B}_u$	3.20	3.58	3.43	3.37
	$1^1\text{B}_u$	6.53	6.76 (4.2)	6.67 (4.4)	6.45
	$2^1\text{A}_g$	7.28	7.14	6.81	6.58
$\text{C}_6\text{H}_8$	$1^3\text{B}_u$	2.64	3.01	2.83	2.77
	$1^1\text{B}_u$	5.60	5.89 (6.5)	5.74 (8.1)	5.59
	$2^1\text{A}_g$	6.55	4.21	5.73	5.58

<sup>a</sup> Also shown are the excitation energies from the semistochastic heat-bath CI (SHCI) method, extrapolated to full CI limit.<sup>111</sup> The  $1s$  orbitals of carbon atoms were not included in the SHCI correlation treatment. The SHCI computations used the same basis sets and optimized geometries as those used for LR-OLCCD, LR-ODC-12, and EOM-CCSD.

for the  $1^1\text{B}_u$  state. Very recently, Chien et al.<sup>111</sup> reported accurate vertical excitation energies for the low-lying states of ethylene, butadiene, and hexatriene computed using semistochastic heat-bath configuration interaction (SHCI) extrapolated to the full CI limit. In this section, we will use the SHCI results to benchmark the accuracy of the LR-ODC-12 method.

Table 4 reports the vertical excitation energies of ethylene, butadiene, and hexatriene computed using the EOM-CCSD, LR-OLCCD, and LR-ODC-12 methods, along with the SHCI results from Ref. 111. All methods employed the same optimized geometries and basis sets (see Table 4 for details). We refer to the  $\text{B}_{1u}$  states of  $\text{C}_2\text{H}_4$  as  $\text{B}_u$  for brevity. All excitation energies decrease as the number of double bonds in a molecule increases. For butadiene and hexatriene, the ( $1^1\text{B}_u$ ;  $2^1\text{A}_g$ ) excitation energies computed using the SHCI method are (6.45; 6.58) and (5.59; 5.58) eV, respectively, indicating that the two states are nearly degenerate for the longer polyene. This feature is not reproduced by the EOM-CCSD method, which predicts the  $1^1\text{B}_u$  state energies in close

agreement with SHCI, but significantly overestimates the energies for the doubly-excited  $2^1\text{A}_g$  state. As a result, the EOM-CCSD method overestimates the energy spacing between the  $1^1\text{B}_u$  and  $2^1\text{A}_g$  states by  $\sim 0.6$  eV and 1.0 eV for butadiene and hexatriene, respectively.

The LR-ODC-12 method, by contrast, correctly describes the relative energies and ordering of the  $1^1\text{B}_u$  and  $2^1\text{A}_g$  states, predicting their energy spacing to be 0.14 and  $-0.01$  eV for butadiene and hexatriene, respectively, in an excellent agreement with the SHCI results (0.13 and  $-0.01$  eV). For the singlet excited states, the LR-ODC-12 method consistently overestimates the SHCI excitation energies by  $\sim 0.1 - 0.2$  eV. For the  $1^3\text{B}_u$  state, the LR-ODC-12 errors are smaller in magnitude ( $\sim 0.06$  eV). Importantly, these results suggest that the LR-ODC-12 method provides a balanced description of the excited states with different electronic structure effects, as illustrated by its consistent performance for the  $1^3\text{B}_u$ ,  $1^1\text{B}_u$ , and  $2^1\text{A}_g$  states in ethylene, butadiene, and hexatriene.

Comparing to LR-OLCCD shows that includ-

ing the non-linear terms in LR-ODC-12 is crucial for the description of excited states with double-excitation character. While for the  $1^3B_u$  and  $1^1B_u$  states the LR-OLCCD errors exceed the LR-ODC-12 errors by  $\sim 0.15$  eV, for the doubly-excited  $2^1A_g$  state the LR-OLCCD errors are much worse: 0.56 and  $-1.37$  eV for butadiene and hexatriene, respectively.

## 5 Conclusions

We have presented a new approach for excited electronic states based on the linear-response formulation of density cumulant theory (DCT). The resulting linear-response DCT model (LR-DCT) has the same computational scaling as the original (single-state) DCT formulation but can accurately predict energies and properties for many electronic states, simultaneously. We have described the general formulation of LR-DCT, derived equations for the linear-response ODC-12 method (LR-ODC-12), and presented its implementation. In LR-ODC-12, excited-state energies are obtained by solving the generalized eigenvalue equation that involves a symmetric Hessian matrix. This simplifies the computation of the excited-state properties (such as transition dipoles) and ensures that the excitation energies have real values, provided that the Hessian is positive semi-definite. In addition, the LR-ODC-12 excitation energies are size-intensive, which we have verified numerically for a system of noninteracting fragments.

Our preliminary results demonstrate that LR-ODC-12 yields very accurate excitation energies for a variety of excited states with different electronic structure effects. For a set of small molecules ( $N_2$ , CO, HCN, HNC,  $C_2H_2$ , and  $H_2CO$ ), LR-ODC-12 outperforms equation-of-motion coupled cluster theory with single and double excitations (EOM-CCSD), with mean absolute errors in excitation energies of less than 0.1 eV, relative to reference data. Importantly, both LR-ODC-12 and EOM-CCSD have the same computational scaling. In a study of ethylene, butadiene, and hexatriene, we have compared the performance of LR-ODC-12 and EOM-CCSD with the results from

highly-accurate semistochastic heat-bath configuration interaction (SHCI). For butadiene and hexatriene, LR-ODC-12 provides a balanced description of the singly-excited  $1^1B_u$  and the doubly-excited  $2^1A_g$  states, predicting that the two states become nearly-degenerate in hexatriene, in excellent agreement with SHCI. By contrast, EOM-CCSD drastically overestimates the energy of the  $2^1A_g$  state, resulting in a  $\sim 1$  eV error in the energy gap between these states of hexatriene.

Overall, our results demonstrate that linear-response density cumulant theory is a promising theoretical approach for spectroscopic properties of molecules and encourage its further development. Several research directions are worth exploring. One of them is the efficient implementation of LR-ODC-12 and its applications to chemical systems with challenging electronic states. Two classes of systems that are particularly worth exploring are open-shell molecules and transition metal complexes. Another direction is to extend LR-DCT to simulations of other spectroscopic properties, such as photoelectron or X-ray absorption spectra. In this regard, applying LR-DCT to the computation of optical rotation properties is of particular interest as it is expected to avoid gauge invariance problems due to the variational nature of the DCT orbitals.<sup>127</sup> We plan to explore these directions in the future.

## A Derivatives of the One-Body Density Matrix in Density Cumulant Theory

Repeated differentiation of the one-body  $n$ -representability condition (Eq. (3)) gives the following formulas for the first and second derivatives of the cumulant partial trace:

$$\frac{\partial \lambda_{qr}^{pr}}{\partial y} = \gamma_s^p \frac{\partial \gamma_q^s}{\partial y} + \frac{\partial \gamma_s^p}{\partial y} \gamma_q^s - \frac{\partial \gamma_q^p}{\partial y} \quad (32)$$

$$\begin{aligned} \frac{\partial^2 \lambda_{qr}^{pr}}{\partial x \partial y} = & \gamma_s^p \frac{\partial \gamma_q^s}{\partial x \partial y} + \frac{\partial \gamma_s^p}{\partial x \partial y} \gamma_q^s - \frac{\partial \gamma_q^p}{\partial x \partial y} \\ & + \frac{\partial \gamma_s^p}{\partial x} \frac{\partial \gamma_q^s}{\partial y} + \frac{\partial \gamma_q^s}{\partial x} \frac{\partial \gamma_s^p}{\partial y} \end{aligned} \quad (33)$$

Transforming to the natural spin-orbital basis (NSO, denoted by prime indices) where the one-body density matrix is diagonal, the first and second derivatives of the one-body density matrix can be determined from the cumulant derivatives as follows:

$$\frac{\partial \gamma_{q'}^{p'}}{\partial y} = \theta_{p'q'} \frac{\partial \lambda_{q'r}^{p'r}}{\partial y} \quad (34)$$

$$\begin{aligned} \frac{\partial^2 \gamma_{q'}^{p'}}{\partial x \partial y} = & \theta_{p'q'} \frac{\partial^2 \lambda_{q'r}^{p'r}}{\partial x \partial y} - \delta_{r'}^{s'} \theta_{p'q'} \theta_{p's'} \theta_{q'r'} \frac{\partial \lambda_{s't}^{p't}}{\partial x} \frac{\partial \lambda_{q'u}^{r'u}}{\partial y} \\ & - \delta_{r'}^{s'} \theta_{p'q'} \theta_{p's'} \theta_{q'r'} \frac{\partial \lambda_{q'u}^{r'u}}{\partial x} \frac{\partial \lambda_{s't}^{p't}}{\partial y} \end{aligned} \quad (35)$$

Here, we have defined the following matrix:

$$\theta_{p'q'} \equiv \begin{cases} (\gamma_{p'} + \gamma_{q'} - 1)^{-1} & \text{if } p', q' \in \text{occ or vir} \\ 0 & \text{otherwise} \end{cases} \quad (36)$$

where  $\gamma_{p'}$  denotes an eigenvalue of the one-body density matrix (i.e., an occupation number). The natural spin-orbital  $p'$  is considered occupied if  $\gamma_{p'} > 0.5$ .

Eqs. (34) and (35) can be used to derive expression for the two-body energy Hessian in Eq. (23). Simplifying the resulting equations allows us to determine the intermediates defined in Eq. (24). In the NSO basis, these intermediates are given by

$$\mathcal{F}_{p'}^{q'} \equiv \theta_{p'q'} f_{p'}^{q'} \quad (37)$$

$$\mathcal{G}_{p'r'}^{q's'} \equiv \theta_{p'q'} \theta_{r's'} (\bar{g}_{p'r'}^{q's'} - \mathcal{F}_{p'}^{s'} \delta_{r'}^{q'} - \mathcal{F}_{r'}^{q'} \delta_{p'}^{s'}) \quad (38)$$

These quantities are computed in the NSO basis and back-transformed to the original spin-orbital basis using the eigenvectors of the one-particle density matrix (see Ref. 53 for more details).

## Acknowledgement

A.V.C. was supported by NSF grant CHE-1661604. A.Y.S. was supported by start-up funds provided by the Ohio State University.

## Supporting Information Available

The following files are available free of charge.

Formulas for the energy Hessian (**E**), the metric matrix (**M**), and the property gradient vector (**v'**) for the LR-ODC-12 and LR-OLCCD methods are included in the Supporting Information.

## References

- (1) Knowles, P. J.; Werner, H.-J. An efficient second-order MC SCF method for long configuration expansions. *Chem. Phys. Lett.* **1985**, *115*, 259–267.
- (2) Wolinski, K.; Sellers, H. L.; Pulay, P. Consistent generalization of the Møller-Plesset partitioning to open-shell and multiconfigurational SCF reference states in many-body perturbation theory. *Chem. Phys. Lett.* **1987**, *140*, 225–231.
- (3) Hirao, K. Multireference Møller–Plesset method. *Chem. Phys. Lett.* **1992**, *190*, 374–380.
- (4) Finley, J.; Malmqvist, P. Å.; Roos, B. O.; Serrano-Andrés, L. The multi-state CASPT2 method. *Chem. Phys. Lett.* **1998**, *288*, 299–306.
- (5) Andersson, K.; Malmqvist, P. Å.; Roos, B. O.; Sadlej, A. J.; Wolinski, K. Second-order perturbation theory with a CASSCF reference function. *J. Phys. Chem.* **1990**, *94*, 5483–5488.
- (6) Andersson, K.; Malmqvist, P. Å.; Roos, B. O. Second-order perturbation theory with a complete active space

- self-consistent field reference function. *J. Chem. Phys.* **1992**, *96*, 1218–1226.
- (7) Angeli, C.; Cimiraglia, R.; Evangelisti, S.; Leininger, T.; Malrieu, J.-P. P. Introduction of  $n$ -electron valence states for multireference perturbation theory. *J. Chem. Phys.* **2001**, *114*, 10252–10264.
  - (8) Angeli, C.; Cimiraglia, R.; Malrieu, J.-P. P.  $N$ -electron valence state perturbation theory: a fast implementation of the strongly contracted variant. *Chem. Phys. Lett.* **2001**, *350*, 297–305.
  - (9) Mukherjee, D.; Moitra, R. K.; Mukhopadhyay, A. Applications of a non-perturbative many-body formalism to general open-shell atomic and molecular problems: calculation of the ground and the lowest  $\pi$ - $\pi^*$  singlet and triplet energies and the first ionization potential of trans-butadiene. *Mol. Phys.* **1977**, *33*, 955–969.
  - (10) Jeziorski, B.; Monkhorst, H. J. Coupled-cluster method for multideterminantal reference states. *Phys. Rev. A* **1981**, *24*, 1668–1681.
  - (11) Werner, H.-J.; Knowles, P. J. An efficient internally contracted multiconfiguration–reference configuration interaction method. *J. Chem. Phys.* **1988**, *89*, 5803–5814.
  - (12) Mahapatra, U. S.; Datta, B.; Mukherjee, D. A state-specific multi-reference coupled cluster formalism with molecular applications. *Mol. Phys.* **1998**, *94*, 157–171.
  - (13) Pittner, J. Continuous transition between Brillouin–Wigner and Rayleigh–Schrödinger perturbation theory, generalized Bloch equation, and Hilbert space multireference coupled cluster. *J. Chem. Phys.* **2003**, *118*, 10876.
  - (14) Evangelista, F. A.; Allen, W. D.; Schaefer, H. F. Coupling term derivation and general implementation of state-specific multireference coupled cluster theories. *J. Chem. Phys.* **2007**, *127*, 024102.
  - (15) Datta, D.; Kong, L.; Nooijen, M. A state-specific partially internally contracted multireference coupled cluster approach. *J. Chem. Phys.* **2011**, *134*, 214116–214116–19.
  - (16) Evangelista, F. A.; Gauss, J. An orbital-invariant internally contracted multireference coupled cluster approach. *J. Chem. Phys.* **2011**, *134*, 114102.
  - (17) Köhn, A.; Hanauer, M.; Mück, L. A.; Jagau, T.-C.; Gauss, J. State-specific multireference coupled-cluster theory. *WIREs Comput. Mol. Sci.* **2013**, *3*, 176–197.
  - (18) Nooijen, M.; Demel, O.; Datta, D.; Kong, L.; Shamasundar, K. R.; Lotrich, V.; Huntington, L. M.; Neese, F. Communication: Multireference equation of motion coupled cluster: A transform and diagonalize approach to electronic structure. *J. Chem. Phys.* **2014**, *140*, 081102.
  - (19) Foresman, J. B.; Head-Gordon, M.; Pople, J. A.; Frisch, M. J. Toward a systematic molecular orbital theory for excited states. *J. Phys. Chem.* **1992**, *96*, 135–149.
  - (20) Sherrill, C. D.; Schaefer, H. F. The Configuration Interaction Method: Advances in Highly Correlated Approaches. *Adv. Quant. Chem.* **1999**, *34*, 143–269.
  - (21) Geertsen, J.; Rittby, M.; Bartlett, R. J. The equation-of-motion coupled-cluster method: Excitation energies of Be and CO. *Chem. Phys. Lett.* **1989**, *164*, 57–62.
  - (22) Comeau, D. C.; Bartlett, R. J. The equation-of-motion coupled-cluster method. Applications to open- and closed-shell reference states. *Chem. Phys. Lett.* **1993**, *207*, 414–423.

- (23) Stanton, J. F.; Bartlett, R. J. The equation of motion coupled-cluster method. A systematic biorthogonal approach to molecular excitation energies, transition probabilities, and excited state properties. *J. Chem. Phys.* **1993**, *98*, 7029.
- (24) Krylov, A. I. Equation-of-Motion Coupled-Cluster Methods for Open-Shell and Electronically Excited Species: The Hitchhiker’s Guide to Fock Space. *Annu. Rev. Phys. Chem.* **2008**, *59*, 433–462.
- (25) Crawford, T. D.; Schaefer, H. F. An Introduction to Coupled Cluster Theory for Computational Chemists. *Rev. Comp. Chem.* **2000**, *14*, 33–136.
- (26) Shavitt, I.; Bartlett, R. J. *Many-Body Methods in Chemistry and Physics*; Cambridge University Press: Cambridge, UK, 2009.
- (27) Sekino, H.; Bartlett, R. J. A linear response, coupled-cluster theory for excitation energy. *Int. J. Quantum Chem.* **1984**, *26*, 255–265.
- (28) Koch, H.; Jensen, H. J. A.; Jørgensen, P.; Helgaker, T. Excitation energies from the coupled cluster singles and doubles linear response function (CCSDLR). Applications to Be, CH<sup>+</sup>, CO, and H<sub>2</sub>O. *J. Chem. Phys.* **1990**, *93*, 3345–3350.
- (29) Koch, H.; Jørgensen, P. Coupled cluster response functions. *J. Chem. Phys.* **1990**, *93*, 3333–3344.
- (30) Nooijen, M.; Bartlett, R. J. A new method for excited states: Similarity transformed equation-of-motion coupled-cluster theory. *J. Chem. Phys.* **1997**, *106*, 6441–6448.
- (31) Nooijen, M.; Bartlett, R. J. Similarity transformed equation-of-motion coupled-cluster theory: Details, examples, and comparisons. *J. Chem. Phys.* **1997**, *107*, 6812–6830.
- (32) Nakatsuji, H.; Hirao, K. Cluster expansion of the wavefunction. Symmetry-adapted-cluster expansion, its variational determination, and extension of open-shell orbital theory. *J. Chem. Phys.* **1978**, *68*, 2053–2065.
- (33) Nakatsuji, H. Cluster expansion of the wavefunction. Electron correlations in ground and excited states by SAC (symmetry-adapted-cluster) and SAC CI theories. *Chem. Phys. Lett.* **1979**, *67*, 329–333.
- (34) Stanton, J. F. Many-body methods for excited state potential energy surfaces. I. General theory of energy gradients for the equation-of-motion coupled-cluster method. *J. Chem. Phys.* **1993**, *99*, 8840–8847.
- (35) Stanton, J. F.; Gauss, J. Analytic energy gradients for the equation-of-motion coupled-cluster method: Implementation and application to the HCN/HNC system. *J. Chem. Phys.* **1994**, *100*, 4695–4698.
- (36) Stanton, J. F.; Gauss, J. Analytic energy derivatives for ionized states described by the equation-of-motion coupled cluster method. *J. Chem. Phys.* **1994**, *101*, 8938–8944.
- (37) Levchenko, S. V.; Wang, T.; Krylov, A. I. Analytic gradients for the spin-conserving and spin-flipping equation-of-motion coupled-cluster models with single and double substitutions. *J. Chem. Phys.* **2005**, *122*, 224106.
- (38) Hättig, C. Structure Optimizations for Excited States with Correlated Second-Order Methods: CC2 and ADC(2). *Adv. Quant. Chem.* **2005**, *50*, 37 – 60.
- (39) Köhn, A.; Tajti, A. Can coupled-cluster theory treat conical intersections? *J. Chem. Phys.* **2007**, *127*, 044105.
- (40) Kjørstad, E. F.; Myhre, R. H.; Martínez, T. J.; Koch, H. Crossing

- conditions in coupled cluster theory. *J. Chem. Phys.* **2017**, *147*, 164105.
- (41) Schirmer, J. Beyond the random-phase approximation: A new approximation scheme for the polarization propagator. *Phys. Rev. A* **1982**, *26*, 2395–2416.
  - (42) Schirmer, J. Closed-form intermediate representations of many-body propagators and resolvent matrices. *Phys. Rev. A* **1991**, *43*, 4647.
  - (43) Dreuw, A.; Wormit, M. The algebraic diagrammatic construction scheme for the polarization propagator for the calculation of excited states. *WIREs Comput. Mol. Sci.* **2014**, *5*, 82–95.
  - (44) Taube, A. G.; Bartlett, R. J. New perspectives on unitary coupled-cluster theory. *Int. J. Quantum Chem.* **2006**, *106*, 3393–3401.
  - (45) Kats, D.; Usvyat, D.; Schütz, M. Second-order variational coupled-cluster linear-response method: A Hermitian time-dependent theory. *Phys. Rev. A* **2011**, *83*, 062503.
  - (46) Wälz, G.; Kats, D.; Usvyat, D.; Korona, T.; Schütz, M. Application of Hermitian time-dependent coupled-cluster response Ansätze of second order to excitation energies and frequency-dependent dipole polarizabilities. *Phys. Rev. A* **2012**, *86*, 052519.
  - (47) Kjønstad, E. F.; Koch, H. Resolving the Notorious Case of Conical Intersections for Coupled Cluster Dynamics. *J. Phys. Chem. Lett.* **2017**, *8*, 4801–4807.
  - (48) Moszynski, R.; Żuchowski, P. S.; Jeziorski, B. Time-Independent Coupled-Cluster Theory of the Polarization Propagator. *Collect. Czech. Chem. Commun.* **2005**, *70*, 1109–1132.
  - (49) Korona, T. XCC2—a new coupled cluster model for the second-order polarization propagator. *Phys. Chem. Chem. Phys.* **2010**, *12*, 14977–14984.
  - (50) Kutzelnigg, W. Density-cumulant functional theory. *J. Chem. Phys.* **2006**, *125*, 171101.
  - (51) Simmonett, A. C.; Wilke, J. J.; Schaefer, H. F.; Kutzelnigg, W. Density cumulant functional theory: First implementation and benchmark results for the DCFT-06 model. *J. Chem. Phys.* **2010**, *133*, 174122.
  - (52) Sokolov, A. Y.; Wilke, J. J.; Simmonett, A. C.; Schaefer, H. F. Analytic gradients for density cumulant functional theory: The DCFT-06 model. *J. Chem. Phys.* **2012**, *137*, 054105–054105–7.
  - (53) Sokolov, A. Y.; Simmonett, A. C.; Schaefer, H. F. Density cumulant functional theory: The DC-12 method, an improved description of the one-particle density matrix. *J. Chem. Phys.* **2013**, *138*, 024107–024107–9.
  - (54) Sokolov, A. Y.; Schaefer, H. F. Orbital-optimized density cumulant functional theory. *J. Chem. Phys.* **2013**, *139*, 204110–204110.
  - (55) Sokolov, A. Y.; Schaefer, H. F.; Kutzelnigg, W. Density cumulant functional theory from a unitary transformation: N-representability, three-particle correlation effects, and application to O4+. *J. Chem. Phys.* **2014**, *141*, 074111.
  - (56) Wang, X.; Sokolov, A. Y.; Turney, J. M.; Schaefer, H. F. Spin-Adapted Formulation and Implementation of Density Cumulant Functional Theory with Density-Fitting Approximation: Application to Transition Metal Compounds. *J. Chem. Theory Comput.* **2016**, *12*, 4833–4842.
  - (57) We note that early on DCT was referred to as “density cumulant functional theory” (DCFT).
  - (58) Fulde, P. *Electron Correlations in Molecules and Solids*; Springer: Berlin, 1991.



- (59) Ziesche, P. Definition of exchange based on cumulant expansion: Correlation induced narrowing of the exchange hole. *Solid State Commun* **1992**, *82*, 597–602.
- (60) Kutzelnigg, W.; Mukherjee, D. Normal order and extended Wick theorem for a multiconfiguration reference wave function. *J. Chem. Phys.* **1997**, *107*, 432.
- (61) Mazziotti, D. A. Approximate solution for electron correlation through the use of Schwinger probes. *Chem. Phys. Lett.* **1998**, *289*, 419–427.
- (62) Mazziotti, D. A. Contracted Schrödinger equation: Determining quantum energies and two-particle density matrices without wave functions. *Phys. Rev. A* **1998**, *57*, 4219–4234.
- (63) Kutzelnigg, W.; Mukherjee, D. Cumulant expansion of the reduced density matrices. *J. Chem. Phys.* **1999**, *110*, 2800–2809.
- (64) Ziesche, P. In *Many-Electron Densities and Reduced Density Matrices*; Cioslowski, J., Ed.; Springer US: Boston, MA, 2000; pp 33–56.
- (65) Herbert, J. M.; Harriman, J. E. Cumulants, Extensivity, and the Connected Formulation of the Contracted Schrödinger Equation. *Adv. Chem. Phys.* **2007**, *134*, 261.
- (66) Kong, L.; Valeev, E. F. A novel interpretation of reduced density matrix and cumulant for electronic structure theories. *J. Chem. Phys.* **2011**, *134*, 214109–214109–9.
- (67) Hanauer, M.; Köhn, A. Meaning and magnitude of the reduced density matrix cumulants. *Chem. Phys.* **2012**, *401*, 50–61.
- (68) Colmenero, F.; Valdemoro, C. Approximating q-order reduced density matrices in terms of the lower-order ones. II. Applications. *Phys. Rev. A* **1993**, *47*, 979–985.
- (69) Nakatsuji, H.; Yasuda, K. Direct Determination of the Quantum-Mechanical Density Matrix Using the Density Equation. *Phys. Rev. Lett.* **1996**, *76*, 1039–1042.
- (70) Mazziotti, D. A. Anti-Hermitian Contracted Schrödinger Equation: Direct Determination of the Two-Electron Reduced Density Matrices of Many-Electron Molecules. *Phys. Rev. Lett.* **2006**, *97*, 143002.
- (71) Kollmar, C. A size extensive energy functional derived from a double configuration interaction approach: The role of N representability conditions. *J. Chem. Phys.* **2006**, *125*, 084108.
- (72) DePrince, A. E.; Mazziotti, D. A. Parametric approach to variational two-electron reduced-density-matrix theory. *Phys. Rev. A* **2007**, *76*, 042501.
- (73) DePrince, A. E. Variational optimization of the two-electron reduced-density matrix under pure-state N-representability conditions. *J. Chem. Phys.* **2016**, *145*, 164109.
- (74) Mazziotti, D. A. Parametrization of the Two-Electron Reduced Density Matrix for its Direct Calculation without the Many-Electron Wave Function. *Phys. Rev. Lett.* **2008**, *101*, 253002.
- (75) Mazziotti, D. A. Parametrization of the two-electron reduced density matrix for its direct calculation without the many-electron wave function: Generalizations and applications. *Phys. Rev. A* **2010**, *81*, 062515.
- (76) DePrince, A. E.; Mazziotti, D. A. Connection of an elementary class of parametric two-electron reduced-density-matrix methods to the coupled electron-pair approximations. *Mol. Phys.* **2012**, *110*, 1917–1925.

- (77) Kutzelnigg, W. Error analysis and improvements of coupled-cluster theory. *Theor. Chem. Acc.* **1991**, *80*, 349–386.
- (78) Kutzelnigg, W. Almost variational coupled cluster theory. *Mol. Phys.* **1998**, *94*, 65–71.
- (79) Van Voorhis, T.; Head-Gordon, M. Benchmark variational coupled cluster doubles results. *J. Chem. Phys.* **2000**, *113*, 8873.
- (80) Kutzelnigg, W. Quantum chemistry in Fock space. I. The universal wave and energy operators. *J. Chem. Phys.* **1982**, *77*, 3081–3097.
- (81) Bartlett, R. J.; Kucharski, S. A.; Noga, J. Alternative coupled-cluster ansätze II. The unitary coupled-cluster method. *Chem. Phys. Lett.* **1989**, *155*, 133–140.
- (82) Watts, J. D.; Trucks, G. W.; Bartlett, R. J. The unitary coupled-cluster approach and molecular properties. Applications of the UCC(4) method. *Chem. Phys. Lett.* **1989**, *157*, 359–366.
- (83) Szalay, P. G.; Nooijen, M.; Bartlett, R. J. Alternative ansätze in single reference coupled-cluster theory. III. A critical analysis of different methods. *J. Chem. Phys.* **1995**, *103*, 281–298.
- (84) Cooper, B.; Knowles, P. J. Benchmark studies of variational, unitary and extended coupled cluster methods. *J. Chem. Phys.* **2010**, *133*, 234102.
- (85) Evangelista, F. A. Alternative single-reference coupled cluster approaches for multireference problems: The simpler, the better. *J. Chem. Phys.* **2011**, *134*, 224102–224102–13.
- (86) Nakata, M.; Yasuda, K. Size extensivity of the variational reduced-density-matrix method. *Phys. Rev. A* **2009**, *80*, 042109.
- (87) Van Aggelen, H.; Verstichel, B.; Bultinck, P.; Van Neck, D.; Ayers, P. W.; Cooper, D. L. Chemical verification of variational second-order density matrix based potential energy surfaces for the N[<sub>sub</sub> 2] isoelectronic series. *J. Chem. Phys.* **2010**, *132*, 114112.
- (88) Verstichel, B.; Van Aggelen, H.; Van Neck, D.; Ayers, P. W.; Bultinck, P. Subsystem constraints in variational second order density matrix optimization: Curing the dissociative behavior. *J. Chem. Phys.* **2010**, *132*, 114113.
- (89) Scheiner, A. C.; Scuseria, G. E.; Rice, J. E.; Lee, T. J.; Schaefer, H. F. Analytic evaluation of energy gradients for the single and double excitation coupled cluster (CCSD) wave function: Theory and application. *J. Chem. Phys.* **1987**, *87*, 5361–5373.
- (90) Salter, E. A.; Trucks, G. W.; Bartlett, R. J. Analytic energy derivatives in many-body methods. I. First derivatives. *J. Chem. Phys.* **1989**, *90*, 1752–1766.
- (91) Gauss, J.; Stanton, J. F.; Bartlett, R. J. Coupled-cluster open-shell analytic gradients: Implementation of the direct product decomposition approach in energy gradient calculations. *J. Chem. Phys.* **1991**, *95*, 2623.
- (92) Gauss, J.; Lauderdale, W. J.; Stanton, J. F.; Watts, J. D.; Bartlett, R. J. Analytic energy gradients for open-shell coupled-cluster singles and doubles (CCSD) calculations using restricted open-shell Hartree–Fock (ROHF) reference functions. *Chem. Phys. Lett.* **1991**, *182*, 207–215.
- (93) Copan, A. V.; Sokolov, A. Y.; Schaefer, H. F. Benchmark Study of Density Cumulant Functional Theory: Thermochemistry and Kinetics. *J. Chem. Theory Comput.* **2014**, *10*, 2389–2398.

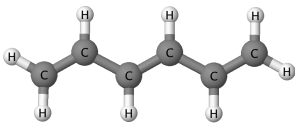
- (94) Mullinax, J. W.; Sokolov, A. Y.; Schaefer, H. F. Can Density Cumulant Functional Theory Describe Static Correlation Effects? *J. Chem. Theory Comput.* **2015**, *11*, 2487–2495.
- (95) Bozkaya, U.; Sherrill, C. D. Orbital-optimized coupled-electron pair theory and its analytic gradients: Accurate equilibrium geometries, harmonic vibrational frequencies, and hydrogen transfer reactions. *J. Chem. Phys.* **2013**, *139*, 054104–054104–12.
- (96) Norman, P. A Perspective on Nonresonant and Resonant Electronic Response Theory for Time-Dependent Molecular Properties. *Phys. Chem. Chem. Phys.* **2011**, *13*, 20519–20535.
- (97) Helgaker, T.; Coriani, S.; Jørgensen, P.; Kristensen, K.; Olsen, J.; Ruud, K. Recent Advances in Wave Function-Based Methods of Molecular-Property Calculations. *Chem. Rev.* **2012**, *112*, 543–631.
- (98) Kristensen, K.; Kauczor, J.; Kjærgaard, T.; Jørgensen, P. Quasienergy Formulation of Damped Response Theory. *J. Chem. Phys.* **2009**, *131*, 044112.
- (99) Olsen, J.; Jørgensen, P. Linear and Nonlinear Response Functions for an Exact State and for an MCSCF State. *J. Chem. Phys.* **1985**, *82*, 3235–3264.
- (100) Sauer, S. P. A. *Molecular Electromagnetism: A Computational Chemistry Approach*; Oxford University Press: Oxford, 2011.
- (101) Parrish, R. M.; Burns, L. A.; Smith, D. G. A.; Simmonett, A. C.; DePrince, A. E.; Hohenstein, E. G.; Bozkaya, U.; Sokolov, A. Y.; Di Remigio, R.; Richard, R. M.; Gonthier, J. F.; James, A. M.; McAlexander, H. R.; Kumar, A.; Saitow, M.; Wang, X.; Pritchard, B. P.; Verma, P.; Schaefer, H. F.; Patkowski, K.; King, R. A.; Valeev, E. F.; Evangelista, F. A.; Turney, J. M.; Crawford, T. D.; Sherrill, C. D. Psi4.1: An Open-Source Electronic Structure Program Emphasizing Automation, Advanced Libraries, and Interoperability. *J. Chem. Theory Comput.* **2017**, *13*, 3185–3197.
- (102) Sun, Q.; Berkelbach, T. C.; Blunt, N. S.; Booth, G. H.; Guo, S.; Li, Z.; Liu, J.; McClain, J. D.; Sayfutyarova, E. R.; Sharma, S.; Wouters, S.; Chan, G. K.-L. PySCF: the Python-based simulations of chemistry framework. *WIREs Comput. Mol. Sci.* **2018**, *8*, e1340.
- (103) Davidson, E. R. The Iterative Calculation of a Few of the Lowest Eigenvalues and Corresponding Eigenvectors of Large Real-Symmetric Matrices. *J. Comput. Phys.* **1975**, *17*, 87–94.
- (104) Liu, B. *The Simultaneous Expansion Method for the Iterative Solution of Several of the Lowest-Lying Eigenvalues and Corresponding Eigenvectors of Large Real-Symmetric Matrices*; 1978; pp 49–53.
- (105) Shao, Y.; Gan, Z.; Epifanovsky, E.; Gilbert, A. T.; Wormit, M.; Kussmann, J.; Lange, A. W.; Behn, A.; Deng, J.; Feng, X.; Ghosh, D.; Goldey, M.; Horn, P. R.; Jacobson, L. D.; Kaliman, I.; Khaliullin, R. Z.; Ku, T.; Landau, A.; Liu, J.; Proynov, E. I.; Rhee, Y. M.; Richard, R. M.; Rohrdanz, M. A.; Steele, R. P.; Sundstrom, E. J.; III, H. L. W.; Zimmerman, P. M.; Zuev, D.; Albrecht, B.; Alguire, E.; Austin, B.; Beran, G. J. O.; Bernard, Y. A.; Berquist, E.; Brandhorst, K.; Bravaya, K. B.; Brown, S. T.; Casanova, D.; Chang, C.-M.; Chen, Y.; Chien, S. H.; Closser, K. D.; Crittenden, D. L.; Didenhofen, M.; Jr., R. A. D.; Do, H.; Dutoi, A. D.; Edgar, R. G.; Fatehi, S.; Fusti-Molnar, L.; Ghysels, A.; Golubeva-Zadorozhnaya, A.; Gomes, J.; Hanson-Heine, M. W.; Harbach, P. H.; Hauser, A. W.; Hohenstein, E. G.; Holden, Z. C.; Jagau, T.-C.;

- Ji, H.; Kaduk, B.; Khistyayev, K.; Kim, J.; Kim, J.; King, R. A.; Klunzinger, P.; Kosenkov, D.; Kowalczyk, T.; Krauter, C. M.; Lao, K. U.; Laurent, A. D.; Lawler, K. V.; Levchenko, S. V.; Lin, C. Y.; Liu, F.; Livshits, E.; Lochan, R. C.; Luenser, A.; Manohar, P.; Manzer, S. F.; Mao, S.-P.; Mardirossian, N.; Marenich, A. V.; Maurer, S. A.; Mayhall, N. J.; Neuscamman, E.; Oana, C. M.; Olivares-Amaya, R.; O'Neill, D. P.; Parkhill, J. A.; Perrine, T. M.; Peverati, R.; Prociuk, A.; Rehn, D. R.; Rosta, E.; Russ, N. J.; Sharada, S. M.; Sharma, S.; Small, D. W.; Sodt, A.; Stein, T.; Stck, D.; Su, Y.-C.; Thom, A. J.; Tsuchimochi, T.; Vanovschi, V.; Vogt, L.; Vydrov, O.; Wang, T.; Watson, M. A.; Wenzel, J.; White, A.; Williams, C. F.; Yang, J.; Yeganeh, S.; Yost, S. R.; You, Z.-Q.; Zhang, I. Y.; Zhang, X.; Zhao, Y.; Brooks, B. R.; Chan, G. K.; Chipman, D. M.; Cramer, C. J.; III, W. A. G.; Gordon, M. S.; Hehre, W. J.; Klamt, A.; III, H. F. S.; Schmidt, M. W.; Sherrill, C. D.; Truhlar, D. G.; Warshel, A.; Xu, X.; Aspuru-Guzik, A.; Baer, R.; Bell, A. T.; Besley, N. A.; Chai, J.-D.; Dreuw, A.; Dunietz, B. D.; Furlani, T. R.; Gwaltney, S. R.; Hsu, C.-P.; Jung, Y.; Kong, J.; Lambrecht, D. S.; Liang, W.; Ochsenfeld, C.; Rassolov, V. A.; Slipchenko, L. V.; Subotnik, J. E.; Voorhis, T. V.; Herbert, J. M.; Krylov, A. I.; Gill, P. M.; Head-Gordon, M. Advances in molecular quantum chemistry contained in the Q-Chem 4 program package. *Mol. Phys.* **2015**, *113*, 184–215.
- (106) Kállay, M.; Rolik, Z.; Csontos, J.; Nagy, P.; Samu, G.; Mester, D.; Csóka, J.; Szabó, B.; Ladjnszki, I.; Szegedy, L.; Ladóczki, B.; Petrov, K.; Farkas, M.; Mezei, P. D.; Hgely., B. MRCC, a quantum chemical program suite. See also: Z. Rolik, L. Szegedy, I. Ladjanszki, B. Ladóczki, and M. Kállay, *J. Chem. Phys.* **139**, 094105 (2013), as well as: [www.mrcc.hu](http://www.mrcc.hu).
- (107) Kendall, R. A.; Dunning Jr, T. H.; Harrison, R. J. Electron affinities of the first-row atoms revisited. Systematic basis sets and wave functions. *J. Chem. Phys.* **1992**, *96*, 6796–6806.
- (108) Widmark, P.-O.; Malmqvist, P. Å.; Roos, B. O. Density matrix averaged atomic natural orbital (ANO) basis sets for correlated molecular wave functions. *Theoret. Chim. Acta* **1990**, *77*, 291–306.
- (109) Daday, C.; Smart, S.; Booth, G. H.; Alavi, A.; Filippi, C. Full Configuration Interaction Excitations of Ethene and Butadiene: Resolution of an Ancient Question. *J. Chem. Theory Comput.* **2012**, *8*, 4441–4451.
- (110) Zimmerman, P. M. Singlet–Triplet Gaps through Incremental Full Configuration Interaction. *J. Phys. Chem. A* **2017**, *121*, 4712–4720.
- (111) Chien, A. D.; Holmes, A. A.; Otten, M.; Umrigar, C. J.; Sharma, S.; Zimmerman, P. M. Excited States of Methylene, Polyenes, and Ozone from Heat-Bath Configuration Interaction. *J. Phys. Chem. A* **2018**, *122*, 2714–2722.
- (112) Tavan, P.; Schulten, K. The low-lying electronic excitations in long polyenes: A PPP-MRD-CI study. *J. Chem. Phys.* **1986**, *85*, 6602–6609.
- (113) Tavan, P.; Schulten, K. Electronic excitations in finite and infinite polyenes. *Phys. Rev. B* **1987**, *36*, 4337–4358.
- (114) Nakayama, K.; Nakano, H.; Hirao, K. Theoretical study of the  $\pi \rightarrow \pi^*$  excited states of linear polyenes: The energy gap between 11Bu+ and 21Ag– states and their character. *Int. J. Quantum Chem.* **1998**, *66*, 157–175.
- (115) Davidson, E. R. The Spatial Extent of the V State of Ethylene and Its Relation

- to Dynamic Correlation in the Cope Rearrangement. *J. Phys. Chem.* **1996**, *100*, 6161–6166.
- (116) Watts, J. D.; Gwaltney, S. R.; Bartlett, R. J. Coupled-cluster calculations of the excitation energies of ethylene, butadiene, and cyclopentadiene. *J. Chem. Phys.* **1998**, *105*, 6979–6988.
- (117) Müller, T.; Dallos, M.; Lischka, H. The ethylene 11B1uV state revisited. *J. Chem. Phys.* **1999**, *110*, 7176–7184.
- (118) Li, X.; Paldus, J. Size dependence of the X1Ag $\rightarrow$ 11Bu excitation energy in linear polyenes. *Int. J. Quantum Chem.* **1999**, *74*, 177–192.
- (119) Starcke, J. H.; Wormit, M.; Schirmer, J.; Dreuw, A. How much double excitation character do the lowest excited states of linear polyenes have? *Chem. Phys.* **2006**, *329*, 39–49.
- (120) Kurashige, Y.; Nakano, H.; Nakao, Y.; Hirao, K. The  $\pi\rightarrow\pi^*$  excited states of long linear polyenes studied by the CASCI-MRMP method. *Chem. Phys. Lett.* **2004**, *400*, 425–429.
- (121) Ghosh, D.; Hachmann, J.; Yanai, T.; Chan, G. K.-L. Orbital optimization in the density matrix renormalization group, with applications to polyenes and  $\beta$ -carotene. *J. Chem. Phys.* **2008**, *128*, 144117.
- (122) Sokolov, A. Y.; Guo, S.; Ronca, E.; Chan, G. K.-L. Time-dependent N-electron valence perturbation theory with matrix product state reference wavefunctions for large active spaces and basis sets: Applications to the chromium dimer and all-trans polyenes. *J. Chem. Phys.* **2017**, *146*, 244102.
- (123) Schreiber, M.; Silva-Junior, M. R.; Sauer, S. P. A.; Thiel, W. Benchmarks for electronically excited states: CASPT2, CC2, CCSD, and CC3. *J. Chem. Phys.* **2008**, *128*, 134110.
- (124) Zgid, D.; Ghosh, D.; Neuscamman, E.; Chan, G. K.-L. A study of cumulant approximations to n-electron valence multireference perturbation theory. *J. Chem. Phys.* **2009**, *130*, 194107.
- (125) Angeli, C. An analysis of the dynamic  $\sigma$  polarization in the V state of ethene. *Int. J. Quantum Chem.* **2010**, *110*, 2436–2447.
- (126) Watson, M. A.; Chan, G. K.-L. Excited States of Butadiene to Chemical Accuracy: Reconciling Theory and Experiment. *J. Chem. Theory Comput.* **2012**, *8*, 4013–4018.
- (127) Lindh, G. D.; Mach, T. J.; Crawford, T. D. The optimized orbital coupled cluster doubles method and optical rotation. *Chem. Phys.* **2012**, *401*, 125–129.

# Graphical TOC Entry

Linear-response density cumulant theory (LR-DCT)  
accurately describes challenging excited states in polyenes:

hexatriene ( $C_6H_8$ )		$1^1B_u$ , eV	$2^1A_g$ , eV
	EOM-CCSD	5.60	6.55
	LR-DCT	5.74	5.73
	Reference	5.59	5.58